CDF/PHYS/TOP/PUBLIC/9427

Top Mass Measurement in the Lepton + Jets Channel Using a Matrix Element Method with Quasi-Monte Carlo Integration and *in situ* Jet Calibration with 2.7 fb^{-1}

The CDF Collaboration
URL http://www-cdf.fnal.gov

(Dated: July 21, 2008)

We report an updated measurement of the top quark mass obtained from $p\bar{p}$ collisions at $\sqrt{s} =$ 1.96 TeV at the Fermilab Tevatron using the CDF II detector. We calculate a signal likelihood using a matrix element integration method with a Quasi-Monte Carlo integration to take into account finite detector resolution and quark mass effects. We use a neural network discriminant to distinguish signal from backgrounds. Our overall signal probability is a 2-D function of m_t and Δ_{JES}, where Δ_{JES} is a shift applied to all jet energies in units of the jet-dependent systematic error. We apply a cut to the peak value of individual event likelihoods in order to reduce the effect of badly reconstructed events. This measurement updates our previous 1.9 fb^{-1} measurement to use 2.7 fb^{-1} of integrated luminosity, requiring events with a lepton, large $\not\!\!E_T$, and exactly four high-energy jets in the pseudorapidity range $|\eta| < 2$. We require that at least one of the jets is tagged as coming from a b quark, and observe 494 total events before and 422 events after applying our likelihood cut. We find $m_t = 172.2 \pm 1.0$ (stat) $\pm$ 0.9 (JES) $\pm$ 1.0 (syst) GeV/c^2, or $m_t = 172.2 \pm 1.7$ (tot) GeV/c^2.

Preliminary Results for Summer 2008 Conferences

I. INTRODUCTION

The top quark mass is an important parameter in the Standard Model, as a precision measurement of the top quark mass (along with the mass of the W boson) provides our best means for constraining the value of the Higgs boson mass. This note describes a precision measurement of the top quark mass performed using a matrix element integration method. For each event we obtain the likelihood of observing that event in our detector as a function of the true top mass m_t by performing a Quasi-Monte Carlo integration over 19 kinematic variables.

This is an update of our previous analysis [1] to use 2.7 fb^{-1} of data collected from $p\bar{p}$ collisions at the Fermilab Tevatron using the CDF II detector, as described in [2]. We search for events in which $t\bar{t}$ pairs are produced, each decays into a W boson and a b quark, and then one W decays into a neutrino and a lepton (meaning, in this paper, an electron or muon) and the other W decays into a $q\bar{q}'$ pair; this is called the "lepton + jets" channel.

We use a neural network constructed from a variety of event variables to distinguish between signal and background events, and employ a cut on the peak likelihood for a given event for additional rejection of background and poorly-modeled events.

The largest systematic uncertainty in the measurement of the top mass is due to uncertainties in the jet energy measurements. A recent technique to deal with this uncertainty consists of introducing a second parameter dealing with the jet energy scale (JES) into the likelihood [1, 3–7], allowing us to use the information contained in the W decay on an event-by-event basis to determine the jet energy scale. Most of the systematic uncertainties on the jet energy scale are thus included in the statistical uncertainty of the result. This technique has proven to significantly reduce the total error due to the JES. In this analysis, we use Δ_{JES}, the shift in the jet energies in units of the jet-specific systematic uncertainty, as our second parameter in our likelihood.

II. DATA AND MONTE CARLO SAMPLES

In this analysis, we identify the top mass candidates in the lepton + jets channel by looking for four high energy jets from the four quarks and a W decay into a lepton and a neutrino. Specifically, for the lepton we require either an electron with $E_T > 20$ GeV or a muon with $p_T > 20$ GeV/c in the central region of the detector. The neutrino is identified by requiring a missing E_T ($\not\!\!E_T$) > 20 GeV in the event. For the jets, we require exactly 4 jets with $E_T > 20$ GeV and pseudorapidity $|\eta| < 2$. The jet p_T has been corrected for inhomogeneities of the detector and nonlinear response of the detector as a function of particle p_T. In addition, at least one of the jets must be tagged as a b-jet using a secondary vertex tagging algorithm.

Background to this signal consists of three main sources: events where a W is produced in conjunction with heavy flavor quarks ($b\bar{b}$, $c\bar{c}$, or c), events where a W is produced along with light quarks which are mistagged, and QCD events that do not contain a W boson but fake a lepton. There are also smaller contributions from diboson, Z, and single top events.

We use a variety of Monte Carlo samples in constructing and evaluating our method. For signal events, we use $t\bar{t}$ events generated at a variety of top masses from 160 GeV/c^2 to 184 GeV/c^2 using the PYTHIA Monte Carlo generator [8]. We also cross-check our analysis using $t\bar{t}$ signal events generated with the HERWIG generator [9]. For W+jets backgrounds, we use Monte Carlo events generated using ALPGEN [10] for the generator and PYTHIA to perform the parton shower. The single top backgrounds use the MadEvent generator [11] and PYTHIA for the parton shower. All Monte Carlo samples are then simulated using the CDFII simulation package. The non-W QCD background is derived from data; for the smaller contributions we do not use Monte Carlo samples, but rather increase the W+light flavor fraction to include diboson and Z contributions. Table I shows the individual contributions. For W+HF and W+LF the background was derived with the method used for the cross section measurement [12], where overlaps in the W+parton samples are removed using the ALPGEN jet-parton matching along with a jet-based heavy flavor overlap removal algorithm. For the 2.7 fb^{-1} sample, the uncertainty on the W+HF background has been increased to account for the increased uncertainty on the K-factor used in this determination.

TABLE I: Expected backgrounds for the W+4 tight jet sample used.

Background	1 tag	$\geq$ 2 tags
non-W QCD	20.0 $\pm$ 17.3	0.8 $\pm$ 1.6
W+light mistag	20.2 $\pm$ 5.6	0.4 $\pm$ 0.1
diboson (WW, WZ, ZZ)	4.5 $\pm$ 0.5	0.4 $\pm$ 0.0
Z $\rightarrow ee, \mu\mu, \tau\tau$	3.0 $\pm$ 0.4	0.3 $\pm$ 0.0
Sum of above 3	27.7 $\pm$ 5.6	1.2 $\pm$ 0.1
W+bb	24.7 $\pm$ 20.2	5.0 $\pm$ 4.2
W+$c\bar{c}$, c	20.3 $\pm$ 17.6	1.0 $\pm$ 0.8
Single top s-chan	1.6 $\pm$ 0.1	0.6 $\pm$ 0.1
Single top t-chan	2.2 $\pm$ 0.1	0.6 $\pm$ 0.1
Sum of above 4	48.8 $\pm$ 13.4	7.2 $\pm$ 2.1
Total background	96.5 $\pm$ 36.8	9.2 $\pm$ 5.2
Predicted top signal	259.4 $\pm$ 33.6	98.8 $\pm$ 16.0
Events observed	389	105

We find that the total number of expected background events in our data sample is $N_{\text{background}} = 105.7 \pm 42.0$ events in 494 observed events.

III. METHOD

For each event we obtain a likelihood distribution as a function of the top pole mass, m_t, and the shift in the jet energy scale, Δ_{JES}. For each jet, the jet energy scale JES is defined by JES $= 1 + \Delta_{\text{JES}} \cdot \sigma(p_T, \eta)$, where $\sigma(p_T, \eta)$ is the relative jet energy scale uncertainty for that jet as estimated by the Jet Corrections Group; the JES is then used as a scale for the jet p_T. The following likelihood expression is used:

$$L(\vec{y} \mid m_t, \Delta_{\text{JES}}) = \frac{1}{N(m_t)} \frac{1}{A(m_t, \Delta_{\text{JES}})} \sum_{i=1}^{24} w_i L_i(\vec{y} \mid m_t, \Delta_{\text{JES}}) \tag{1}$$

with

$$L_i(\vec{y} \mid m_t, \Delta_{\text{JES}}) = \int \frac{f(z_1) f(z_2)}{FF} \, \text{TF}(\vec{y} \mid \vec{x}, \Delta_{\text{JES}}) \, |M(m_t, \vec{x})|^2 \, d\Phi(\vec{x}) \tag{2}$$

where $\vec{y}$ are the quantities we measure (lepton momenta and jet momenta); $\vec{x}$ are the parton-level quantities that define the kinematics of the event; $N(m_t)$ is a global normalization factor; Δ_{JES} is the parameter defining the jet p_T shift; $A(m_t, \Delta_{\text{JES}})$ is the acceptance for $t\bar{t}$ lepton+jets events for the given values of m_t and Δ_{JES}; $f(z_1)$ and $f(z_2)$ are obtained from the momentum probability distributions, *i.e.,* the PDFs, for incoming partons z_1 and z_2; FF is the flux factor for the PDFs; $\text{TF}(\vec{y} \mid \vec{x}, \Delta_{\text{JES}})$ are the transfer functions that predict the measured jet momenta distributions from the parton-level quarks; $d\Phi(\vec{x})$ indicates integration over the phase space of the process including the necessary Jacobians; $\text{M}(m_t, \vec{x})$ is the matrix element for $t\bar{t}$ production and decay; and w_i are the jet permutation weights assigned according to the presence of b tags. Finally we sum over all possible jet permutations.

The PDFs $f(z_1)$ and $f(z_2)$ are integrated over the appropriate combinations of incoming $q\bar{q}$ and gluons. The flux factor acts as a normalization for the PDFs. We use the CTEQ5L PDFs [13] in our integration.

We discuss the further components of the integration in the following sections.

Matrix element: We use the Kleiss-Stirling matrix element [14] which includes both $q\bar{q} \to t\bar{t}$ and $gg \to t\bar{t}$ production processes, as well as all spin correlations.

Integration variables: Assuming that the lepton momentum is well-measured, there are 19 dimensions in the phase space above. In our past analyses [7], we made further assumptions to reduce the integration dimensionality. However, with the usage of Quasi-Monte Carlo integration (discussed further below), we are able to integrate over the full phase space. We choose our set of variables to be the two m_t^2 and m_W^2 on the leptonic and hadronic side of the decay, $\beta = \log(p_1/p_2)$, where p_1 and p_2 are the scalar momenta of the two hadronic W decay products, the two-dimensional vector p_T of the $t\bar{t}$ system, and finally the η, ϕ, and m for each of the four jet-producing partons (which we call "proto-jets").

Quasi-Monte Carlo integration: The Quasi-Monte Carlo integration method differs from standard Monte Carlo integration in that it uses a quasi-random sequence to generate points. Formally, a quasi-random sequence is one with a low discrepancy, where the discrepancy is a measure of the uniformity of the sequence. This allows an improvement in the convergence of the integral over the standard $1/\sqrt{N}$ convergence of standard Monte Carlo integration [15].

We employ QMC integration for 18 of the 19 variables. The leptonic m_W^2 requires special treatment to avoid phase space singularities when $\partial m_W^2/\partial p_z^\nu = 0$, so a grid-based procedure is used in this dimension. Transfer functions are used for the p_T and angles of the jets, while the $p_T(t\bar{t})$ and jet mass variables are integrated over using priors derived from Monte Carlo.

To speed up the integration, we apply importance sampling schemes to many of the integration variables; for instance, the top masses are sampled in the space of the cumulative distributions of their Breit-Wigners. Also, in the permutation sum, less time is spent integrating permutations which are identified to have a lower probability.

Transfer functions: The transfer functions connect the measured jets to the partons. We construct our transfer functions by taking $t\bar{t} \to$ lepton + jets Monte Carlo events in a wide range of masses and matching the simulated jets to their parent partons. In our analysis, we factorize the transfer functions into separate momentum and angular parts. The momentum transfer functions are built as probability distributions of the ratio of the p_T of the jet to the p_T of the parton, while the angular transfer functions are built as probability distributions of $\Delta\eta$ and $\Delta\phi$, which are the differences between the η and ϕ of the jet and the parton. Both the momentum and angular transfer functions are built with dependence on the proto-jet p_T and mass, and there are separate transfer functions built for each of 4 separate bins of jet η as well as for b and light quarks.

Figure 1 shows sample p_T and angular transfer functions.

An additional efficiency factor is also included in the transfer functions to account for the fact that the transfer functions are built from a sample which is inevitably affected by acceptance effects. This factor ensures that the transfer functions are correctly normalized even given these effects.

Normalization: The normalization factor $N(m_t)$ is obtained by integrating the Kleiss-Sterling matrix element together with the PDFs and the flux factor over the phase space formed by the two initial and the six final state particles. Figure 2 shows the normalization used in our analysis, with the HERWIG cross-section included for reference.

Acceptance: The acceptance $A(m_t, \Delta_{\mathrm{JES}})$ is obtained from Monte Carlo events in which we randomize the directions and momenta of the partons to create objects which should look like final-state jets. We do this for all the values of the top mass and Δ_{JES} over which the likelihood function is defined, and then calculate the acceptance at each m_t and Δ_{JES} value to be the fraction of these MC events which pass our selection cuts.

The advantage to this approach as opposed to using fully simulated Monte Carlo is that it does not have events with an incorrect set of jets, and such events are excluded from the efficiency calculations as well. Our probability model describes tree level signal events with the correct set

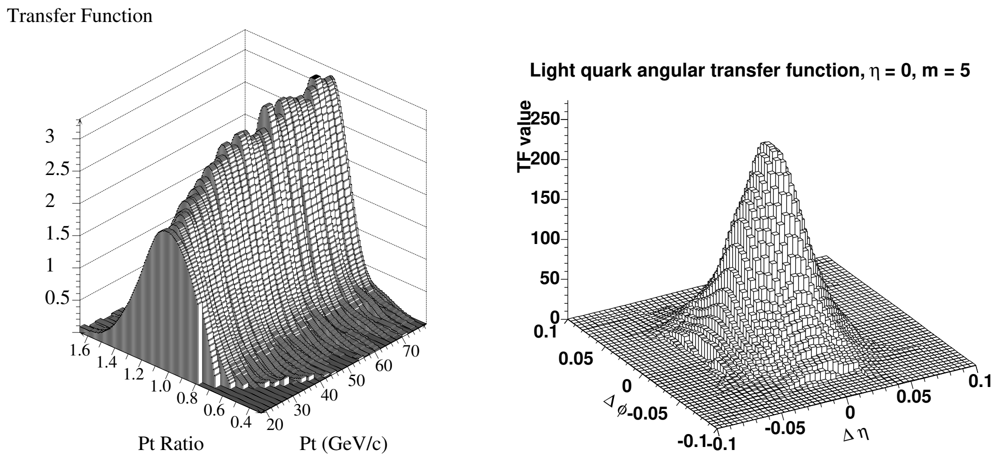

FIG. 1: Sample momentum (left) and angular (right) transfer functions.

of jets; therefore, we cannot use fully simulated events which include effects not included in the model. Furthermore, we can generate our acceptance from a much larger sample of events, reducing statistical fluctuations in the resulting curve. Figure 2 shows the 2-D acceptance as a function of m_t and JES.

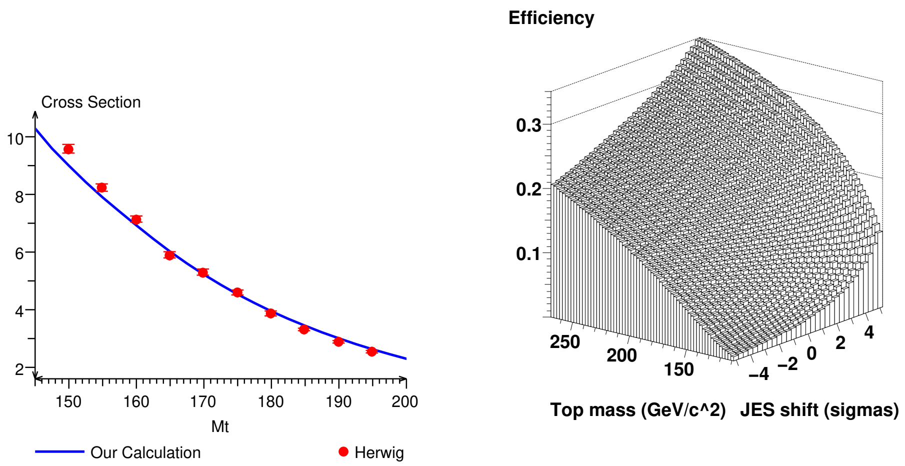

FIG. 2: Normalization and acceptance used in our integration.

IV. BACKGROUND DISCRIMINATION AND HANDLING

Our integration method calculates the likelihood for an event under the assumption that it is a signal event. Therefore, we need a mechanism to reject background events.

We identify background events using a neural network. Our neural network uses ten inputs: the P_T for each of the four leading jets; the E_T of the lepton; the missing E_T, $\not{E}_T$; H_T, the scalar sum of the jet transverse energies, lepton transverse energy, and missing E_T; and three variables

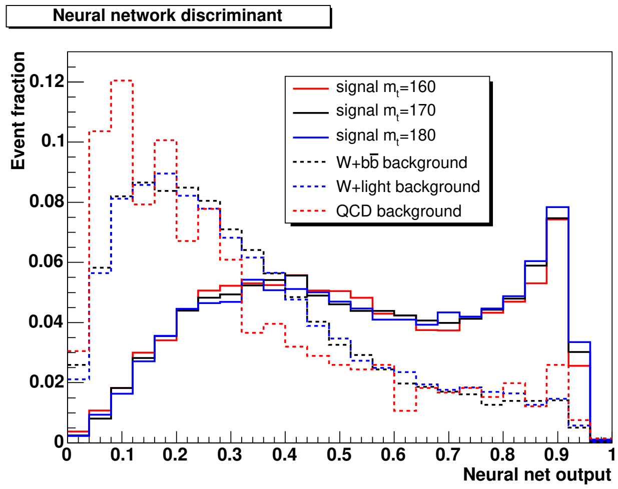

FIG. 3: The distributions of our hybrid variable for signal and background Monte Carlo events. The solid lines indicate signal events at various masses, while the dashed lines indicate various types of backgrounds.

describing the shape of the event: the aplanarity, defined as 3/2 the smallest eigenvalue of the momentum tensor $\Theta_{ab} = \sum_i p_a^i p_b^i / \sum_i |\vec{p_i}|^2$; $D_R = \Delta R_{ij}^{\min} \cdot \min(p_z^{(i,j)})/p_T^{\ell}$, where $\Delta R_{ij}^{\min}$ is the smallest ΔR between any pair of jets; and $H_{\rm TZ} = \sum_{i=2}^4 |p_T^i|/(\sum_{i=1}^4 |p_z^i| + |p_z^\ell| + |p_z^\nu|)$, the ratio of the scalar sums of the transverse momenta (excluding the leading jet) to the longitudinal momenta.

The neural network is trained to separate $t\bar{t}$ events with a mass of 170 GeV/c^2 and $W + b\bar{b}$ background; we then cross-check the neural network with other signal masses and background types to make sure that the output shape is not dependent on the signal mass present.

Figure 3 shows the neural network output for a variety of different samples. We then compute the background fraction for this event as $f_{\rm bg}(q) = B(q)/(B(q) + S(q))$, where the background and signal distributions are normalized to their overall expected fractions.

Next, we need to use this discriminant to remove the background contribution from our total likelihood to recover our signal likelihood. We compute the average likelihood for background events (computed, like all of our events, under the assumption that they are signal) from Monte Carlo and subtract out the expected contribution, where $n_{\rm bg}$ is the expected number of background events:

$$\log L_{\rm tot} = \sum_i (\log L_i) - n_{\rm bg} \log \overline{L(\text{background})}$$

We can rewrite our previous equation in terms of the individual per-event background fraction to obtain our final likelihood formula:

$$\log L_{\rm mod}(m_t, \text{JES}) = \sum_{\text{events}} [\log L(m_t, \text{JES}\,|\text{signal}) - f_{\rm bg}(q) \log \overline{L(m_t, \text{JES}\,|\text{background})}]$$

These two expressions are equivalent if the events follow their expected distributions. However, the advantage to using $f_{\rm bg}$ per event rather than the total of $n_{\rm bg}$ is that if there are more or fewer background events in our sample than expected, $f_{\rm bg}$ should be able to capture some of this change.

In addition, there is another class of undesirable events which is not handled by the above method. These are events in which a $t\bar{t}$ pair is produced, but where the final observed objects in our detector (the jets and lepton) do not all directly come from the $t\bar{t}$ decay. We call these events "bad signal" events. These exist due to a variety of causes (extra jets from gluon radiation,

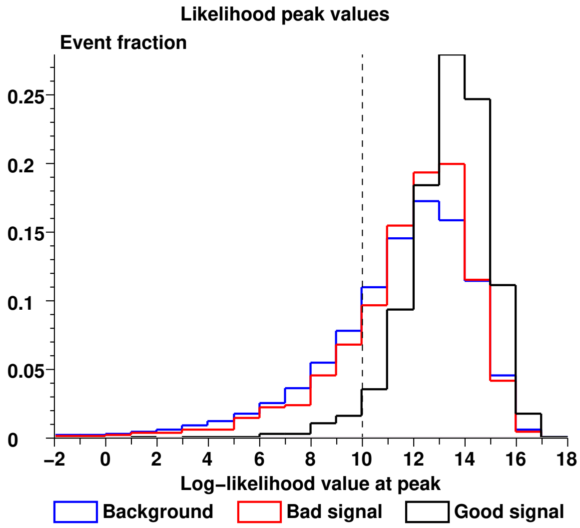

FIG. 4: Distribution of the log-likelihood peak value for "good signal", "bad signal", and background events in Monte Carlo.

misidentified dilepton or all-hadronic events, $W \to \tau$ decay, etc.) and comprise roughly 35% of our total signal (for a signal mass of 172 GeV/c^2, we see that 36.2% of 1-tag and 30.9% of >1-tag events are "bad signal"). In order to deal with these events, we implement a cut of 10 on the log of the value of the peak of the likelihood curve. Table II shows the efficiency of this cut for "good signal" events, "bad signal" events, and background events. Figure 4 shows the distribution of the log-likelihood peak values for the three classes of events in Monte Carlo.

TABLE II: Efficiency of the likelihood cut at a value of 10.

Type of event	Total	1-tag	>1-tag
Good signal	96.6%	95.9%	98.0%
Bad signal	79.6%	79.8%	78.9%
Background	73.4%	73.5%	71.2%

V. TOP MASS EXTRACTION

Our 2-D likelihood gives us the joint likelihood of observing the events that we see as a function of the top mass m_t and the jet energy scale Δ_{JES}. In order to obtain a final result, we treat the Δ_{JES} as a nuisance parameter and eliminate it using the profile likelihood. In the profile likelihood method, we simply take the maximum value of the likelihood along the Δ_{JES} axis for each m_t value. That is:

$$L_{\mathrm{prof}}(m_t) = \max_{j \in \Delta_{\mathrm{JES}}} L(m_t, j)$$

This gives us a 1-D likelihood curve in m_t only. We then follow the normal procedure of taking the peak as our result and descending 1/2 unit of log-likelihood from the peak to determine the uncertainty.

We test our method using Monte Carlo samples of simulated $t\bar{t}$ events and four backgrounds (W+heavy flavor, W+light flavor, QCD, and single top), as described in section II. We construct pseudo-experiments (PEs) from the Monte Carlo using a Poisson average of 427.8 events per pseudo-experiment, the number of events we expect to have after applying the likelihood cut. We run 2000 PEs for each signal top mass value and compute the resulting average measured mass, bias, expected statistical uncertainty, and pull width. Figure 5 shows the results.

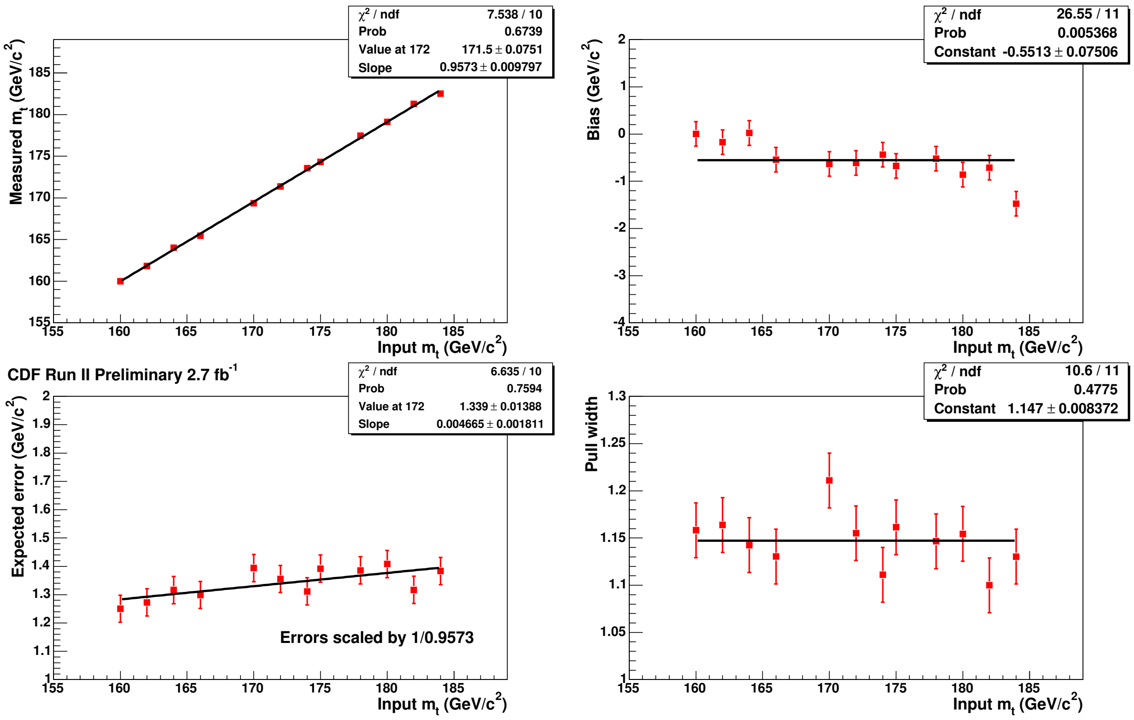

FIG. 5: Pseudoexperiment results using fully simulated signal and background events after applying a likelihood cut, mean of 427.8 events/PE. Top left: reconstructed vs. input top mass; top right: bias vs. input top mass; bottom left: expected uncertainty vs. input top mass; bottom right: pulls vs. input top mass.

We also test and calibrate our measurement by running on samples where the input $\Delta_{\rm JES}$ has been shifted away from its nominal value of 0. Figure 6 shows the results of the $\Delta_{\rm JES}$ measurement for these shifted samples, as well as the dependence of the measured mass on the input $\Delta_{\rm JES}$. We see that there is a small dependence, which we must account for in our final calibration.

Based on the results from these PEs, we determine the calibration for our final measurement. First we use the measured bias and slope for the mass and $\Delta_{\rm JES}$ measurements to calibrate these quantities individually; then, we use the measured slope of the output m_t as a function of $\Delta_{\rm JES}$ as a final correction. Our final calibration formula is thus:

$$\begin{aligned} \Delta m_{\rm calib} &= (\Delta m_{\rm meas} + 0.551)/0.957 - 0.40 \cdot (\Delta_{\rm JES})_{\rm calib} \\ (\Delta_{\rm JES})_{\rm calib} &= ((\Delta_{\rm JES})_{\rm meas} + 0.310)/0.880 \end{aligned}$$

We also correct the measured uncertainties using the slope and pull widths obtained:

$$\begin{aligned} (\sigma_m)_{\rm calib} &= (\sigma_m)_{\rm meas} \times 1.147/0.957 \\ (\sigma_{\Delta_{\rm JES}})_{\rm calib} &= (\sigma_{\Delta_{\rm JES}})_{\rm meas} \times 1.082/0.880 \end{aligned}$$

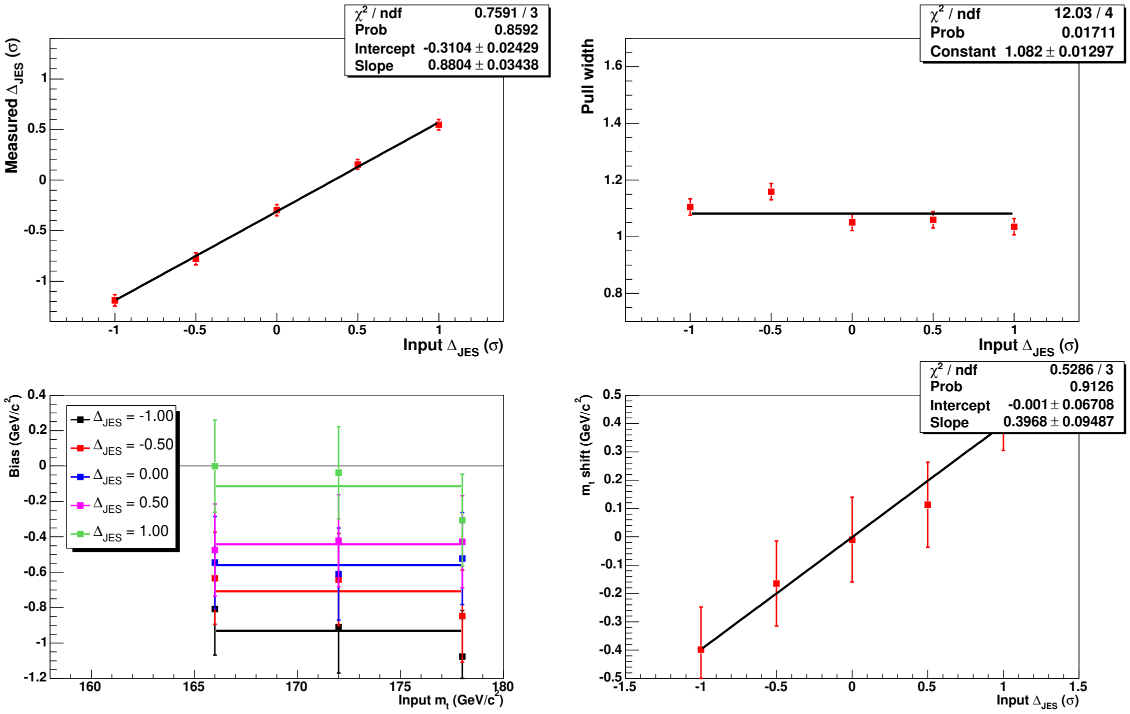

FIG. 6: Pseudoexperiment results using fully simulated signal and background events after applying a likelihood cut, mean of 427.8 events/PE. Top left: measured $\Delta_{\rm JES}$ vs. input $\Delta_{\rm JES}$; top right: $\Delta_{\rm JES}$ pulls vs. input $\Delta_{\rm JES}$; bottom left: measured bias vs. input top mass for different $\Delta_{\rm JES}$ values; bottom right: measured shift in m_t vs. input $\Delta_{\rm JES}$.

VI. RESULTS

In the data we find a total of 422 events which pass all of our cuts (including the likelihood peak cut): 325 1-tag events and 97 >1-tag events. Combining these likelihoods, we use the profile likelihood to extract a top mass value, which we then correct using the previously-described calibration, to measure a mass of 172.2 ± 1.3 GeV$/c^2$. We can use a similar procedure to extract a $\Delta_{\rm JES}$ measurement of $0.09 \pm 0.29\ \sigma$. Figure 7 shows the resulting 2-D likelihood from each subset of the events after the calibration has been applied.

This uncertainty combines both the statistical uncertainty and the uncertainty due to JES uncertainty. To separate these two causes, we take the m_t likelihood in the $\Delta_{\rm JES} = 0$ bin and evaluate the uncertainty in the resulting 1-D likelihood. This yields an uncertainty of 1.0 GeV$/c^2$. Thus, we conclude that the remaining uncertainty of 0.9 GeV$/c^2$ is due to the JES and report a final value of:

$$m_t = 172.2 \pm 1.0\ (\text{stat.}) \pm 0.9\ (\text{JES})\ \text{GeV}/c^2. \tag{3}$$

Figure 8 shows the expected statistical uncertainty from Monte Carlo events at a top mass of 172 GeV$/c^2$, with the measured uncertainty from data shown as the black arrow. 49% of pseudoexperiments show a lower uncertainty than measured in the data.

As a cross-check, Figure 9 shows the comparison of the log-likelihood peak value of the likelihood curves between data and Monte Carlo. A Kolmogorov-Smirnov test on the agreement between the two shows a confidence level of 0.85, showing that the likelihood peak information is well-modeled

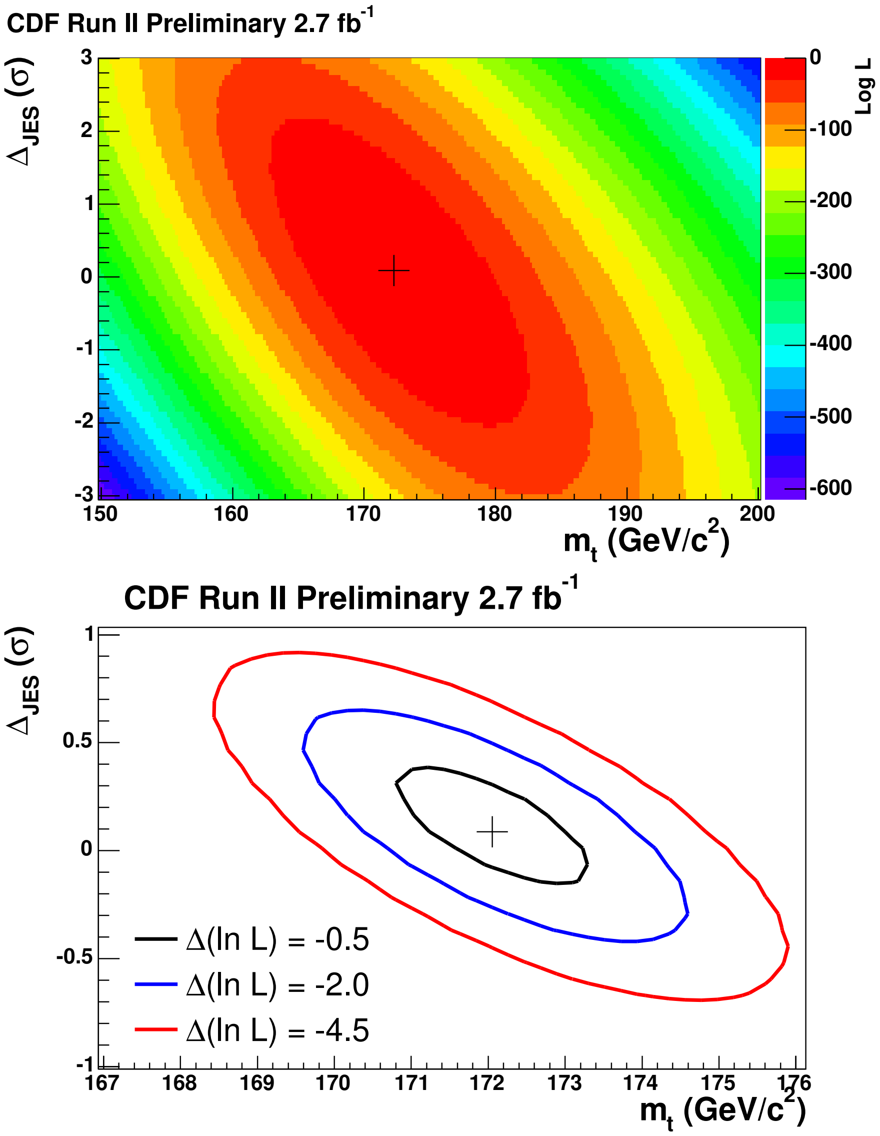

FIG. 7: Measured 2-D likelihood on the data events. The top plot shows the likelihood on the full range used in our integration. The bottom plot shows the contours corresponding to a 1-σ, 2-σ, and 3-σ uncertainty in our measurement. The full 2-D calibration has been applied. The marker shows the point of maximum likelihood.

by Monte Carlo and hence that our likelihood cut procedure is valid.

Our systematics are summarized in Table III. Here is a brief description of the major systematic sources:

We assign a systematic uncertainty for the uncertainty in our calibration constants as described previously.

Our analysis is tested and calibrated on PYTHIA Monte Carlo. We evaluate a systematic due to the generator by comparing the results from HERWIG and PYTHIA samples.

Systematics due to initial-state radiation and final-state radiation are evaluated using Monte Carlo samples where the amount of ISR and FSR has been increased and decreased.

While the 2-D measurement is designed to capture any changes in the Δ_{JES}, the jet energy

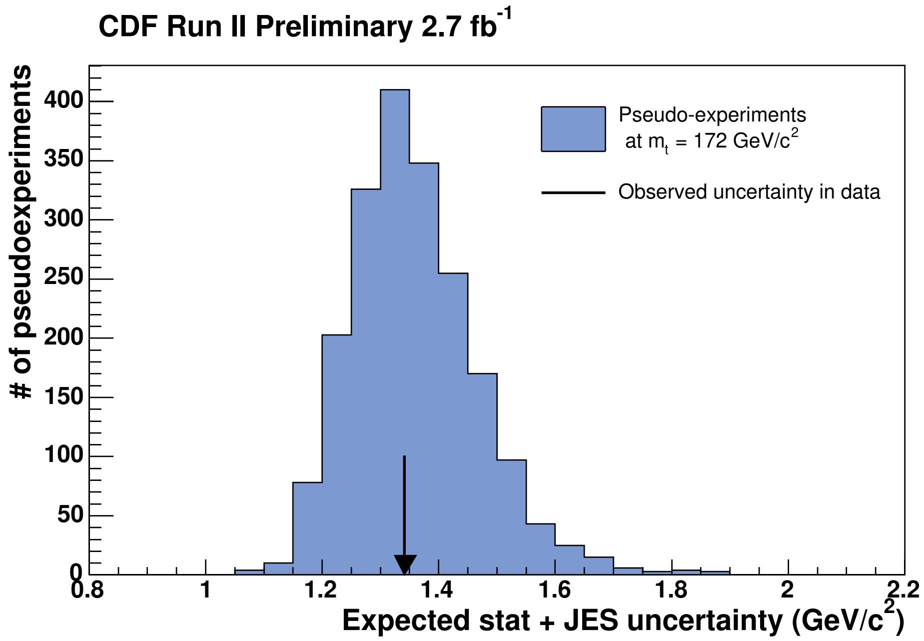

FIG. 8: Expected statistical uncertainty on the 2-D profile likelihood method for $m_t = 172$. The black arrow indicates the measured uncertainty in data. All uncertainties have been calibrated using the measured pull width and slope.

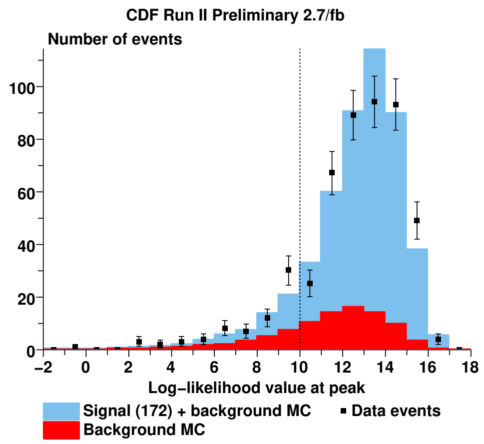

FIG. 9: Comparison of the log-likelihood value of the peak of likelihood curves for data and Monte Carlo.

systematics are derived from several separate sources of uncertainty, which may exhibit different behavior with respect to jet p_T and η than the overall uncertainty. We thus vary the jet energies by one σ for each of the separate sources. The resulting shifts are added in quadrature to obtain our residual JES systematic uncertainty.

We account for additional uncertainties in the jet energy scale for b-jets by considering three sources of uncertainty. First, we measure the uncertainty due to the semileptonic decay fraction by varying it by $\pm 1\sigma$. Second, we measure the the uncertainty due to the b fragmentation model by trying two different b frgamentation models. Thirdly, we measure uncertainty due to differing calorimeter response by varying b-jets in the Monte Carlo by 0.2% and measuring the resulting top mass.

TABLE III: Total list of systematics.

Systematic source	Systematic uncertainty (GeV/c^2)
Calibration	0.1
MC generator	0.5
ISR and FSR	0.3
Residual JES	0.5
b-JES	0.4
Lepton P_T	0.2
Pileup	0.1
PDFs	0.2
Background	0.4
Total	1.0

Since the Monte Carlo has a lower luminosity and hence fewer pileup interactions per event than the most recent data, we evaluate a potential systematic due to this source by measuring the top mass as a function of the number of interactions in the event and multiplying the resulting slope by the difference in the number of interactions between MC and data.

We evaluate the systematics due to the parton distribution functions (PDFs) used in the matrix element integration by comparing different PDF sets (CTEQ5L and MRST72 [16]), varying α_s, and varying the eigenvectors of the CTEQ6M PDFs. This also includes a systematic on the fraction of our events from gg vs. $q\bar{q}$.

There are several uncertainties associated with our background method. First, we vary our overall background fraction by its uncertainty and measure the resulting change in the top mass. Second, we check the background composition by setting our background to 100% $W+b\bar{b}$, $W+c\bar{c}/c$, W + light, or QCD background and measuring the resulting changes. Third, we check the systematics due to our average background likelihood shape by dividing the sample into two subsamples (one with even-numbered events, and one with odd-numbered events), building the average shape from one subsample, and measuring the top mass on the other subsample. Finally, we use background samples with a different Q^2 scale used by the Monte Carlo generator to evaluate the systematics due to this source. We also include an uncertainty for limited background statistics in the MC.

We also have small systematics resulting from the permutation weighting used in our integration and uncertainty in the lepton P_T.

VII. CONCLUSIONS

In conclusion, our measured top quark mass in 2.7 fb^{-1} with 422 events passing all our cuts is:

$$m_t = 172.2 \pm 1.0\ (\text{stat.}) \pm 0.9\ (\text{JES}) \pm 1.0\ (\text{syst.})\ \text{GeV}/c^2$$
$$m_t = 172.2 \pm 1.3\ (\text{stat.}) \pm 1.0\ (\text{syst.}) = 172.2 \pm 1.7\ (\text{total})\ \text{GeV}/c^2.$$

Acknowledgments

We thank the Fermilab staff and the technical staffs of the participating institutions for their vital contributions. This work was supported by the U.S. Department of Energy and National Science Foundation; the Italian Istituto Nazionale di Fisica Nucleare; the Ministry of Education, Culture, Sports, Science and Technology of Japan; the Natural Sciences and Engineering Research Council of Canada; the National Science Council of the Republic of China; the Swiss National Science Foundation; the A.P. Sloan Foundation; the Bundesministerium für Bildung und Forschung, Germany; the Korean Science and Engineering Foundation and the Korean Research Foundation;

the Science and Technology Facilities Council and the Royal Society, UK; the Institut National de Physique Nucleaire et Physique des Particules/CNRS; the Russian Foundation for Basic Research; the Ministerio de Educación y Ciencia and Programa Consolider-Ingenio 2010, Spain; the Slovak R&D Agency; and the Academy of Finland.

---

[1] The CDF Collaboration, "Top Mass Measurement in the Lepton + Jets Channel Using a Matrix Element Method with Quasi-Monte Carlo Integration and *in situ* Jet Calibration with 1.9 fb^{-1}", CDF public note 9301 (April 2008).
[2] F. Abe, et al., Nucl. Instrum. Methods Phys. Res. A **271**, 387 (1988); D. Amidei, et al., Nucl. Instrum. Methods Phys. Res. A **350**, 73 (1994); F. Abe, et al., Phys. Rev. D **52**, 4784 (1995); P. Azzi, et al., Nucl. Instrum. Methods Phys. Res. A **360**, 137 (1995); The CDFII Detector Technical Design Report, Fermilab-Pub-96/390-E
[3] The CDF Collaboration, "Measurement of the Top Quark Mass using the Template Method in the Lepton plus Jets Channel with *In Situ* $W \to jj$ Calibration", Phys. Rev. Lett. **83**, 022004 (2006); CDF public note 8125 (March 2006).
[4] The CDF Collaboration, "Measurement of the Top Quark Mass using the Matrix Element Analysis Technique in the Lepton + Jets Channel with In-Situ $W \to jj$ Calibration", Phys. Rev. Lett. **99**, 182002 (2007; CDF public note 8151 (March 2006).
[5] The CDF Collaboration, "Measurement of the top quark mass in the all hadronic channel using an in-situ calibration of the dijet invariant mass with 943 pb^{-1}", CDF public note 8709 (February 2007).
[6] The CDF Collaboration, "Top Mass Measurement in the Lepton + Jets Channel Using a Multivariate Method and *in situ* Jet Calibration", CDF public note 8780 (April 2007).
[7] The CDF Collaboration, "Top Mass Measurement in the Lepton + Jets Channel Using a Modified Matrix Element Method and *in situ* Jet Calibration", CDF public note 9025 (September 2007); "Top Mass Measurement in the Lepton + Jets Channel Using a Modified Matrix Element Method and *in situ* Jet Calibration with 1.9 fb^{-1}", CDF public note 9196 (February 2008).
[8] PYTHIA version 6.216, T. Sjöstrand, P. Edén, C. Friberg, L. Lönnblad, G. Miu, S. Mrenna and E. Norrbin, Computer Phys. Commun. 135 (2001) 238 (LU TP 00-30, hep-ph/0010017).
[9] HERWIG version 6.510, G. Corcella, I.G. Knowles, G. Marchesini, S. Moretti, K. Odagiri, P. Richardson, M.H. Seymour and B.R. Webber, JHEP 0101 (2001) 010 [hep-ph/0011363]; hep-ph/0210213.
[10] ALPGEN version 2.10 prime, M.L. Mangano, M. Moretti, F. Piccinini, R. Pittau, A. Polosa, JHEP 0307:001,2003, hep-ph/0206293. Note that PYTHIA v6.325 is used for the showering.
[11] MadGraph/MadEvent v4, J. Alwall, P. Demin, S. de Visscher, R. Frederix, M. Herquet, F. Maltoni, T. Plehn, D. Rainwater, T. Stelzer, JHEP 0709:028,2007, arXiv:0706.2334.
[12] The CDF Collaboration, "Measurement of the $t\bar{t}$ Production Cross Section in $p\bar{p}$ collisions at $\sqrt{s} = 1.96$ TeV using Lepton + Jets Events with Secondary Vertex b-tagging", CDF public note 8795 (May 2007).
[13] H. L. Lai *et al.*, Eur. Phys. J. C **12**, 375 (2000).
[14] R. Kleiss and W. J. Stirling, Z. Phys. C **40**, 419 (1988).
[15] W. Morokoff and R. E. Caflisch, "Quasi-Random Sequences and Their Discrepancies", *SIAM Journal of Scientific and Statistical Computing* **15**, 1251-1279 (1994).
[16] A. D. Martin, R. G. Roberts, W. J. Stirling and R. S. Thorne, Eur. Phys. J. C **4**, 463 (1998).